Electromagnetic Fields Mediate Efficient Cell Reprogramming into a Pluripotent State

Soonbong Baek,[†] Xiaoyuan Quan,[†] Soochan Kim,[‡] Christopher Lengner,[§] Jung-Keug Park,[∞] and Jongpil Kim*[,†]

[†]Lab of Stem Cells and Cell Reprogramming, Department of Biomedical Engineering, Dongguk University, Seoul 100-715, Korea, [∞]Dongguk University Research Institute of Biotechnology, Dongguk University, Seoul 100-715, Korea, [‡]Department of Electrical and Electronic Engineering, Hankyong National University, Kyonggi-do 456-749, Korea, and [§]Department of Animal Biology, School of Veterinary Medicine, University of Pennsylvania, Philadelphia, Pennsylvania 19104, United States

ABSTRACT Life on Earth is constantly exposed to natural electromagnetic fields (EMFs), and it is generally accepted that EMFs may exert a variety of effects on biological systems. Particularly, extremely low-frequency electromagnetic fields (EL-EMFs) affect biological processes such as cell development and differentiation; however, the fundamental mechanisms by which EMFs influence these processes remain unclear. Here we show that EMF exposure induces epigenetic changes that promote efficient somatic cell reprogramming to pluripotency. These epigenetic changes resulted from EMF-induced activation of the histone lysine methyltransferase Mll2. Remarkably, an EMF-free system that eliminates Earth's naturally occurring magnetic field abrogates these epigenetic changes, resulting in a failure to undergo reprogramming. Therefore, our results reveal that EMF directly regulates dynamic epigenetic changes through Mll2, providing an efficient tool for epigenetic reprogramming including the acquisition of pluripotency.

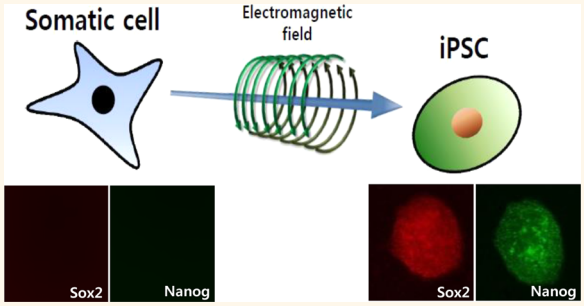

KEYWORDS: electromagnetic fields · cell reprogramming · epigenetic changes

Earth has a magnetic field that extends from its inner core to where it meets the solar wind, protecting us from a stream of cosmic rays emanating from space.[1] Its magnitude at the earth's surface ranges from 25 to 65 μT, and all life on earth has evolved in the presence of this field. In addition to this naturally occurring magnetic field, humans are now exposed to electromagnetic fields (EMFs) more than ever as electrical technology becomes increasingly ubiquitous.[2] Thus, there are growing concerns in public health regarding the potential consequences of increasing exposure to man-made electromagnetic fields.[3−7] Epidemiological studies show that exposure to EMF is associated with a risk of cancer and other diseases.[8,9] However, this myriad of studies suggests that there is a general agreement on the effects of EMFs on biological systems.

For example, it has been suggested that extremely low-frequency electromagnetic fields (EL-EMFs) influence numerous types of changes in cells including migration, cell differentiation, apoptosis, and stress response.[10−15] EL-EMFs also arise at various stages of embryonic development, affecting morphology and migration of embryonic cells.[15−17] Furthermore, it has been reported that a specific frequency of EMFs promotes osteogenic and neurogenic differentiation that has been clinically applied in the repair of bone fractures and to promote wound healing.[18−21] Taken together, these collective studies indicate that EMFs may be involved in governing cell fate conversion, although direct evidence of EMF effects on cell fate plasticity remains lacking.

To examine whether EMFs play critical roles in controlling cell fate changes, we ask whether EMF exposure can influence epigenetic reprogramming by facilitating cell fate conversion. Somatic cells can be reprogrammed to induced pluripotent stem cells (iPSC) by the overexpression of defined factors, most notably the four "Yamanaka factors", Oct4, Sox2, Klf4, and c-Myc.[22]

* Address correspondence to jpkim153@dongguk.edu.

Received for review May 30, 2014 and accepted September 23, 2014.

Published online September 23, 2014
10.1021/nn502923s

© 2014 American Chemical Society

Epigenetic reprogramming embodies the most dramatic change of cellular identity, so this system enables us to study the role of EMFs in governing epigenetic plasticity. Gaining specific insight into how EMFs influence epigenetic identity will provide a foundation for harnessing this phenomenon in directed differentiation protocols and for therapeutic purposes.

Here, we report that EMF exposure results in enhanced reprogramming efficiency in somatic cells. We find that a specific frequency of EMF enhances epigenetic changes during the reprogramming process *via* the induction of Mll2, a histone lysine *N*-methyltransferase, which is known to contribute to the methylation of histone 3 lysine 4 (H3K4me3). Furthermore, we demonstrate a requirement for EMFs in the generation of induced pluripotent stem cells (iPS cells) as EMF inhibition is sufficient to completely abrogate epigenetic changes and cell fate conversion in these systems. Finally, we demonstrate that these EMF-free phenotypes can be rescued by the overexpression of Mll2. Thus, our results suggest that Mll2 mediates EMF-induced reprogramming at the level of the epigenome to drive cell fate change. These results provide a foundation for harnessing this phenomenon in directed cell fate plasticity and therapeutic application.

RESULTS

Specific Frequency of EMF Exposure Enhances Epigenetic Reprogramming of Mouse Somatic Cells. In 2006, Takahashi and Yamanaka achieved nuclear reprogramming of somatic cells to pluripotency through the direct expression of defined transcription factors.[22] The generation of iPS cells *via* direct epigenetic reprogramming provides critical evidence for the plasticity of the somatic epigenome. In order to examine whether EL-EMF can directly influence changes in epigenetic identity, we reprogrammed mouse somatic cells into iPSCs under EMF exposure (Figure 1A). Initially, we transduced mouse tail tip fibroblasts (TTFs) harboring an eGFP reporter at the endogenous *Oct4* locus[23] with a polycistronic doxycycline (dox)-inducible lentiviral vector expressing the Oct4, Sox2, Klf4, and c-Myc (OSKM) transcription factors[24] along with a lentiviral vector constitutively expressing a modified reverse tetracycline transactivator (M2rtTA) (Figure 1A). After infection, dox was introduced and the culture was exposed to varying EL-EMF frequencies (10, 50, and 100 Hz frequencies at 1 mT intensity) (Supporting Information Figure S1A). Remarkably, EL-EMF-treated cultures exhibited an increase in colonies undergoing reprogramming as assessed by alkaline phosphatase (AP) staining, with a maximum increase in efficiency observed 15 days after infection and exposure to 50 Hz, 1 mT EL-EMF (Figure S1A). We quantified the expression of pluripotency-related genes in these assays. EL-EMF exposure during the 2 weeks of dox treatment resulted in a significant increase in the expression of endogenous Oct4, Sox2, and Nanog relative to controls (Figure 1B). The agonistic effects of EL-EMF on pluripotency-related gene expression were specific to cells undergoing reprogramming, as EL-EMF-exposed cells not expressing the four factors did not exhibit any induction of these transcripts (Figure 1B). Specific induction of additional embryonic stem-cell-specific genes such as Esrrb, Fbx15, Rex1, and Zfp296 was observed in EL-EMF-treated cultures (Figure S1B). We confirmed the observed increase in the efficiency of iPSC generation using *Oct4-eGFP* fibroblasts, where EL-EMF resulted in approximately 30-fold increase in the number of *Oct4-eGFP*+ cells (Figure 1C,D). Additionally, we examined reprogramming efficiency using *Nanog-eGFP* knock-in fibroblasts[25] and observed a similar increase in iPSC cell generation with exposure to EL-EMF (50 Hz, 1 mT) relative to controls (Figure S1C). These findings provide clear evidence that exposure to EL-EMF promotes somatic cell reprogramming into pluripotency.

After withdrawal of dox on day 15, *Oct4-eGFP*-positive colonies were stable and expressed pluripotency genes in a manner identical to mouse embryonic stem cells (mESCs) after 50 passages, demonstrating that these iPSCs had reactivated their endogenous pluripotency regulatory network (Supporting Information Figure S1D,E). At the protein level, all dox-independent iPSC lines stably expressed the pluripotency markers Oct4, Nanog, Sox2, and SSEA-1 (Figure 1E), consistent with bisulfite sequence analysis, demonstrating demethylation of the endogenous *Oct4* and *Nanog* promoters in these iPS cells (Figure S2A). Since small molecules such as valproic acid (VPA) and vitamin C (Vc) have been reported to increase efficiency of iPSC generation,[26,27] we compared reprogramming efficiencies between VPA, Vc, and EL-EMF-treated cultures. Strikingly, EL-EMF exposure resulted in the most efficient iPSC formation confirmed by AP staining and Oct4-eGFP activity 15 days after 4 factor induction (Figure 1F and Figure S2B). Teratoma formation analysis confirmed the presence of cell types derived from all three embryonic germ layers, validating the pluripotency of these EL-EMF-induced iPSCs (Figure S2C). Moreover, we tested whether EL-EMF-induced iPSCs are germline competent. High contribution chimeras were generated from these iPSCs and were crossed to C57BL/6J mice. Resulting litters included agouti pups that, together with PCR analysis, demonstrate the germline potential of EL-EMF-induced iPSCs (Figure S2D). Taken together, these results demonstrate that EL-EMF exposure in mouse somatic cells results in significantly increased reprogramming efficiency.

Generation of iPS Cells by Oct4 and EL-EMF Exposure. This robust increase in reprogramming efficiency led us to examine whether EL-EMF exposure could also replace some of the canonical reprogramming factors during iPSC generation. To test this, we prepared dox-inducible one factor (Oct4), two factor (Oct4+Sox2), and control mouse embryonic fibroblasts (MEFs), in either the

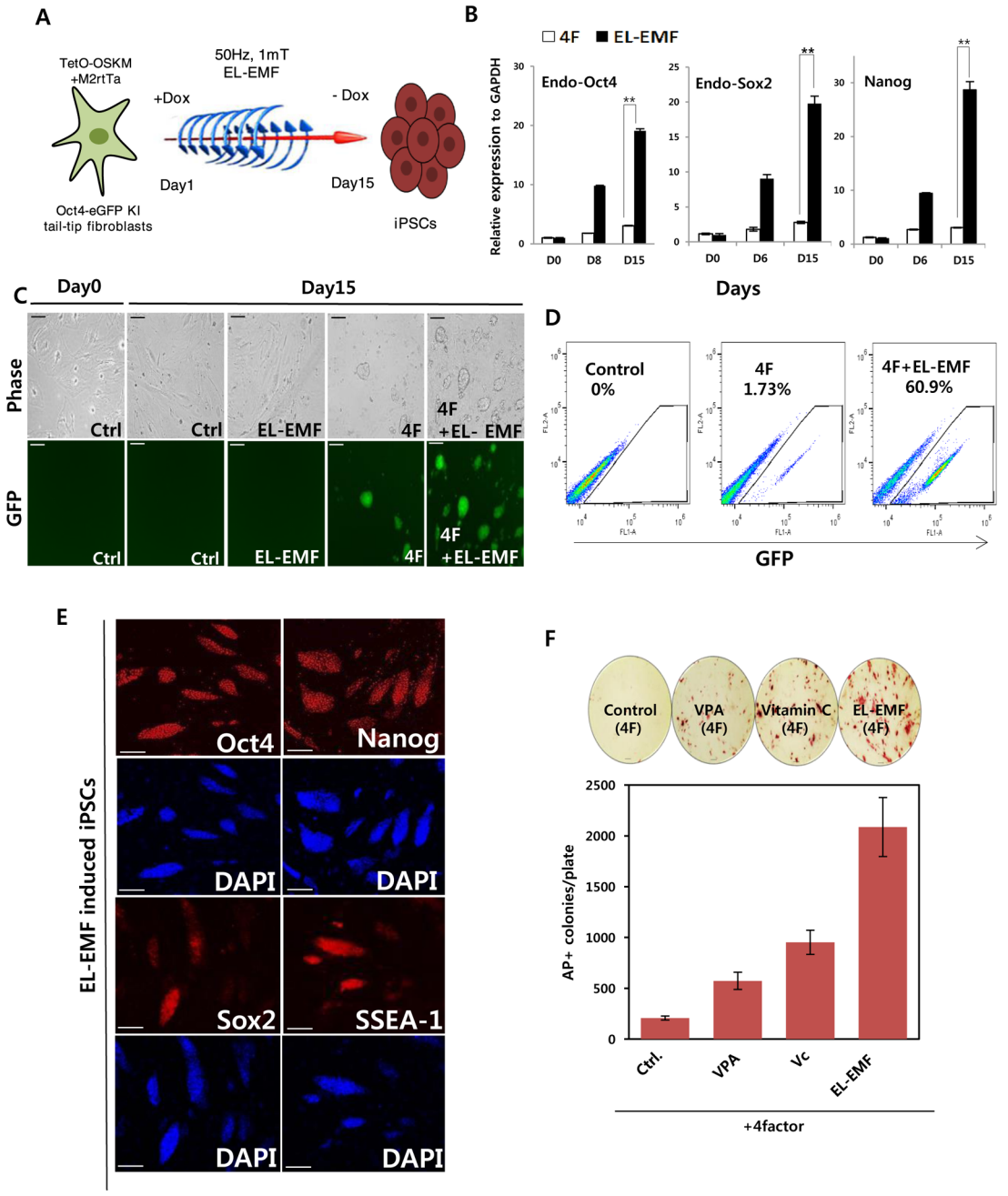

Figure 1. Efficient generation of iPS cells with EL-EMF exposure in mouse somatic cells. (A) Schematic drawing of the cell reprogramming with EL-EMF exposure. (B) RT-PCR analysis of pluripotency markers, Oct4, Sox2, and Nanog of OSKM-infected fibroblasts in the presence and absence of EL-EMF at 6 and 15 days after dox induction. Three independent experiments of three sets each were performed. Data represent mean ± SEM. Student *t* test, **$p < 0.01$. (C) GFP expression in iPSC colonies generated from *Oct4-eGFP* knock-in (KI) fibroblasts in the absence and presence of EL-EMF exposure 15 days after dox treatment (top panel, bright field; bottom panel, fluorescence photograph). Scale bars: 100 μm. (D) FACS analysis for Oct4-GFP+ cells from Oct4-eGFP KI fibroblasts in the absence and presence of EL-EMF exposure at 15 days after dox treatment. (E) Immunostaining of EL-EMF-induced iPSCs (E-iPSC) for the pluripotency markers Oct4, Sox2, Nanog, and SSEA1. Scale bars: 100 μm. (F) Representative image (top) and number of GFP-positive colonies (bottom) from 4 factor reprogramming combined with different conditions: valproic acid (VPA), vitamin C (Vc), and EL-EMF exposure. Equal numbers of 4-factor-infected cells were plated but treated with the different conditions, with EL-EMF exposure resulting in the highest induction of AP+ cells at day 15. Scale bars: 100 μm.

presence or the absence of EL-EMF exposure 30 days after infection, and observed that Oct4 and Sox2 combined with EL-EMF significantly increased the iPSC-like colony formation, indicating that EL-EMF can replace c-Myc and Klf4 efficiently (Supporting Information Figure S3A). Additionally, Oct4 alone combined with EL-EMF exposure induced AP-positive iPSC colonies 30 days after infection (Figure 2A,B), whereas no colonies were observed in the 1- or 2-factor-infected conditions without EL-EMF exposure (Figure S3A and Figure 2B).

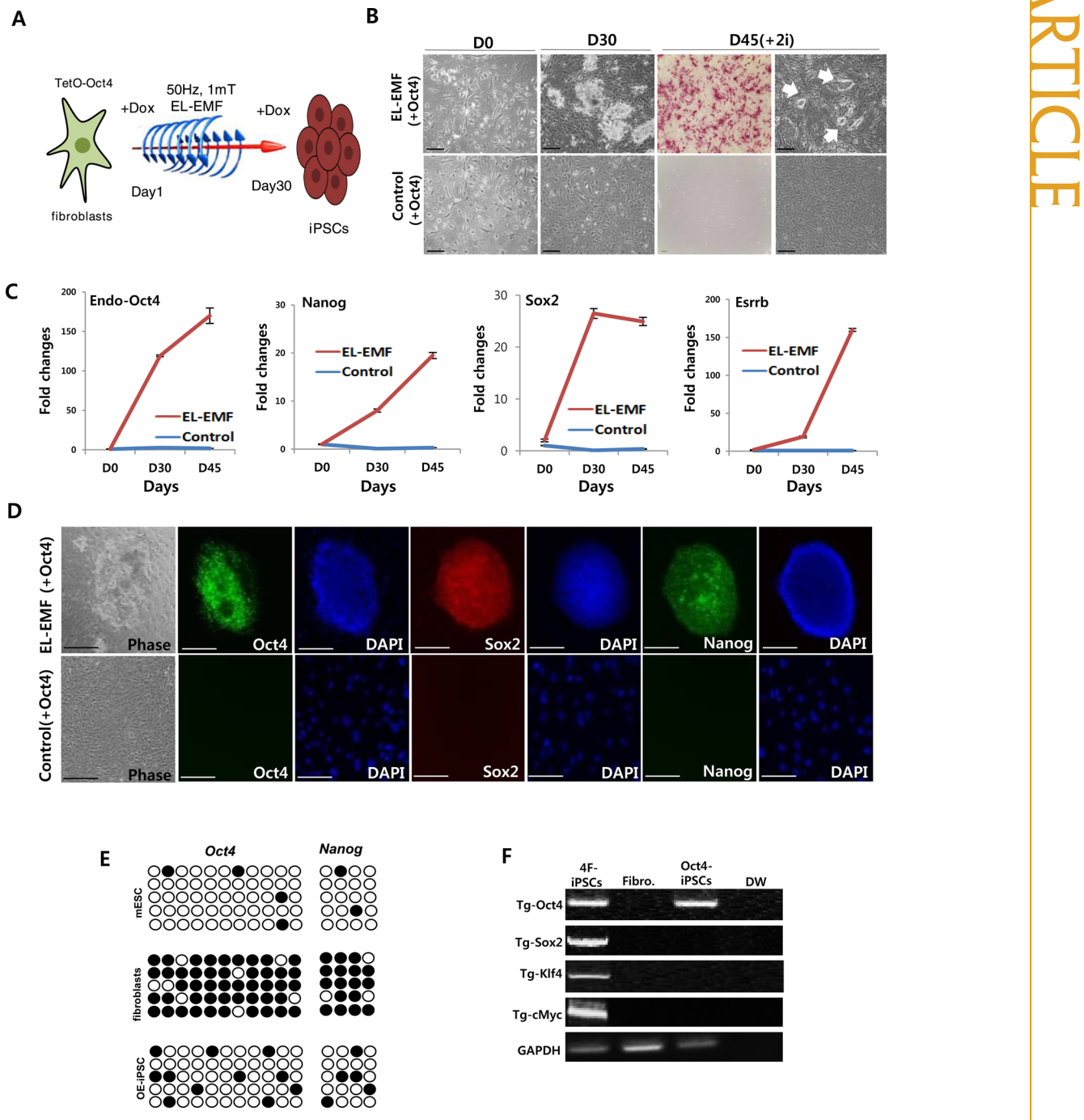

Figure 2. Generation of iPS cells by Oct4 with EL-EMF exposure. (A) Schematic of the strategy of reprogramming by Oct4 alone with EL-EMF. (B) Morphology and AP staining of Oct4 and EL-EMF-induced iPSCs (OE-iPSCs), compared with Oct4-infected fibroblasts, with AP staining 30 and 45 day after infection. Three independent experiments of three sets each were performed. Scale bars: 100 μm. (C) Expression levels of pluripotency markers (Oct4, Sox2, Nanog, and Esrrb) in Oct4- and EL-EMF-induced iPS cells and Oct4-infected fibroblasts. Three independent experiments of three sets each were performed. Data represent mean $\pm$ SEM. (D) Immunofluorescence staining for pluripotency markers (Oct4, Sox2, and Nanog) of Oct4- and EL-EMF-induced iPSCs and Oct4-infected fibroblasts. Scale bars: 100 μm. (E) Bisulfite sequencing of Oct4 and Nanog gene promoters showing the methylation state of Oct4/EL-EMF-induced iPSCs. Open circles indicate unmethylated, and filled circles indicate methylated CpG dinucleotides. (F) Transgene integrations of Oct4- and EL-EMF-induced iPSCs.

Additionally, we observed that treatment with inhibitors of glycogen synthase kinase 3β (GSK3β) and mitogen-activated protein kinase (ERK1/2), known as 2i, in the Oct4 and EL-EMF-induced colonies leads to further upregulation of pluripotency markers and decreases in H3K27me3 level in the cells (Figure 2C and Figure S3B). Forty-five days after infection, all iPS colonies were AP+ (Figure 2B) and expressed the pluripotency markers Nanog, Oct4, and Sox2 (Figure 2D). Bisulfite sequencing of the Oct4 and

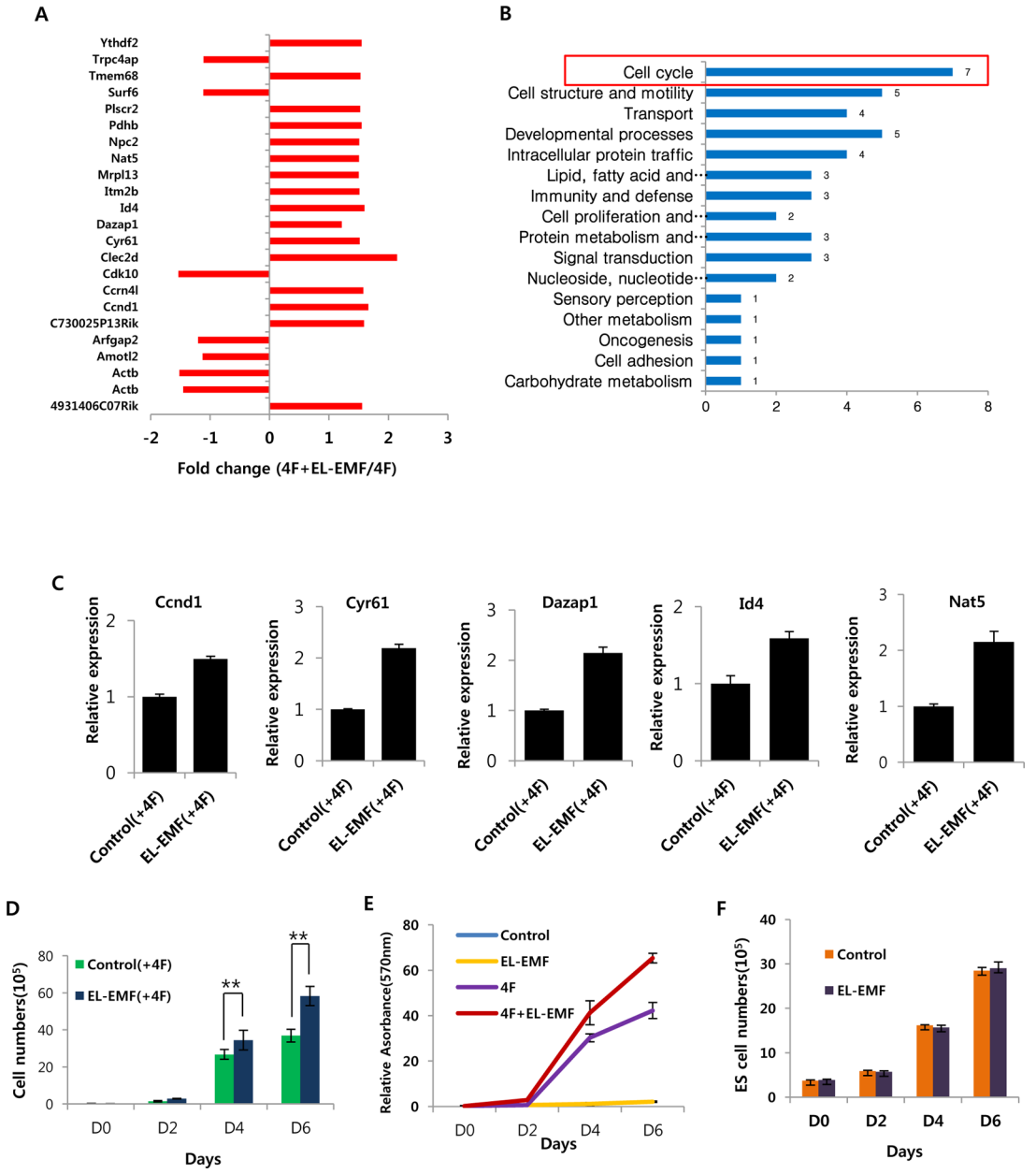

Figure 3. Gene expression analysis of EL-EMF exposure reprogramming. (A) Fold change of differentially expressed genes from global gene expression profiling in the presence and absence of EL-EMF exposure during cell reprogramming. Expression differences are shown in red color. Red bar means 1.5-fold higher or lower expression. (B) GO analysis of differentially expressed genes affected by EL-EMF exposure. (C) qRT-PCR analysis of cell-cycle-related genes, Ccnd1, Cybrb1, Dazac1, Id4, and Nat5. Expression levels were normalized to GAPDH. Data are presented as mean ± SEM; $n = 3$. (D) Growth curves for secondary fibroblasts in the presence or absence of EL-EMF exposure. Three independent experiments of three sets each were performed. Data represent mean ± SEM. Student t test, $^{**}p < 0.01$. (E) MTT assay for cell number of control fibroblasts and secondary fibroblasts during the reprogramming process in the presence and absence of EL-EMF exposure. Three independent experiments of three sets each were performed. Data represent mean ± SEM. (F) Growth curves for ESCs (V6.5) in the presence or absence of EL-EMF exposure.

Nanog promoters showed nearly complete demethylation in Oct4/EL-EMF-induced iPSCs (OE-iPSCs) (Figure 2E). The genomic integration of the Oct4 transgene was confirmed by PCR analysis (Figure 2F). These cells were also competent in chimera formation assays (Figure S2D), demonstrating their pluripotency and indicating that use of the EL-EMF exposure during reprogramming has no adverse effect on the resulting iPSCs. Taken together, these results demonstrate that fibroblasts can be reprogrammed to pluripotency by the forced expression of only one factor, Oct4, with EL-EMF exposure.

Mechanisms of EL-EMF-Induced Cell Reprogramming. To gain insight into the mechanism by which EMF enhances reprogramming, we first assayed global gene expression in cells undergoing reprogramming in

TABLE 1. List of Differentially Expressed Genes of Secondary Fibroblasts in the Presence and Absence of EL-EMF

target ID	gene symbol	panther_function
ILMN_2612325	4931406C07Rik	molecular function unclassified
ILMN_2846865	Actb	cytoskeletal protein → actin family cytoskeletal protein → actin and actin-related protein
ILMN_2588055	Actb	cytoskeletal protein → actin family cytoskeletal protein → actin and actin-related protein
ILMN_2774049	Amotl2	miscellaneous function → other miscellaneous function protein
ILMN_2461696	Arfgap2	nucleic acid binding; select regulatory molecule → G-protein modulator → other G-protein modulator
ILMN_2773862	C730025P13Rik	molecular function unclassified
ILMN_2669793	Ccnd1	select regulatory molecule → kinase modulator → kinase activator
ILMN_1255422	Ccrn4l	nucleic acid binding
ILMN_2646209	Cdk10	kinase → protein kinase → nonreceptor serine/threonine protein kinase
ILMN_2603647	Clec2d	receptor → other receptor; signaling molecule → membrane-bound signaling molecule; defense/immunity protein → other defense and immunity protein
ILMN_2794645	Cyr61	signaling molecule → growth factor
ILMN_2860674	Dazap1	nucleic acid binding → other RNA-binding protein
ILMN_2678714	Id4	transcription factor → other transcription factor
ILMN_2782082	Itm2b	miscellaneous function → other miscellaneous function protein
ILMN_2982200	Mrpl13	nucleic acid binding → ribosomal protein
ILMN_1223543	Nat5	transferase → acetyltransferase
ILMN_2744380	Npc2	molecular function unclassified
ILMN_3116570	Pdhb	oxidoreductase → dehydrogenase
ILMN_2635895	Plscr2	transfer/carrier protein → other transfer/carrier protein
ILMN_2753108	Surf6	nucleic acid binding
ILMN_2602257	Tmem68	molecular function unclassified
ILMN_1225522	Trpc4ap	molecular function unclassified
ILMN_1225360	Ythdf2	molecular function unclassified

the presence of EL-EMF. To ensure rapid and homogeneous induction of cell reprogramming, we prepared inducible secondary MEFs in which all of the cells in the culture harbor the identical site of integration and copy number of dox-inducible reprogramming factors.[28] Reprogramming of secondary MEFs was initiated with dox in the presence or absence of EL-EMF exposure. To assess changes in gene expression induced by EL-EMF, we analyzed the transcriptome of secondary MEFs after EL-EMF exposure and compared the transcriptional profiles to control secondary MEFs. EL-EMF exposure resulted in some changes in global gene expressions (Figure 3A and Table 1). We identified 24 genes whose expression changed after EL-EMF exposure, and gene ontology (GO) analysis across the two independent experimental sets identified an upregulation of gene signatures associated with cell cycle (Figure 3B). Quantitative RT-PCR analysis shows that cell-cycle-related genes, including Ccnd1, Cyr61, Dazac1, Id3, and Nat5, were markedly elevated in EL-EMF-treated cultures in comparison to untreated cultures (Figure 3C). However, these genes are expressed at the same level in ESCs and fibroblasts in the presence or absence of EMF (data not shown). These results suggested that EL-EMF exposure does not significantly affect pluripotent or somatic conditions but may promote cell fate conversion during the reprogramming process. Consistent with this idea, we observed a significant increase in cell proliferation upon EMF exposure in the secondary MEFs but no induction of cell proliferation in fibroblasts and mESC (Figure 3D–F). A previous study has demonstrated that increasing proliferation during reprogramming *via* p53 or p21 inhibition results in accelerated reprogramming.[29] However, the increase in proliferation alone is insufficient to account for the effects of EL-EMF observed in our study as we found EL-EMF capable of replacing Sox2, Klf4, and c-Myc in the reprogramming cocktail and a much greater increase in reprogramming efficiency than can be accounted for by the observed increase in cell proliferation (up to 30-fold efficiency with less than 2-fold increase in proliferation). Thus, we reasoned that EL-EMF enhances the reprogramming process through additional mechanisms.

Direct reprogramming occurs with massive changes to the epigenome, including changes in histone modification and DNA methylation.[30−32] Prior studies demonstrated that EL-EMF exposure can affect chromatin modification.[33,34] Thus, in order to examine whether EL-EMF exposure affects histone modifications during reprogramming, we measured the expression level of histone modifiers in the EL-EMF-exposed secondary fibroblasts. Most histone modifiers were grossly unaffected in EL-EMF-exposed secondary fibroblasts 3 days after dox treatment; however, we observed a dramatic upregulation of the *KMT2D* gene that encodes the lysine-specific methyltransferase myeloid/mixed-lineage leukemia 2 (Mll2) in EL-EMF-exposed cells (Figure 4A,B). Induction of Mll2 precedes upregulation of Oct4 expression in the reprogramming process (Supporting Information Figure S4A), and Mll2 expression is significantly increased at day 6 after

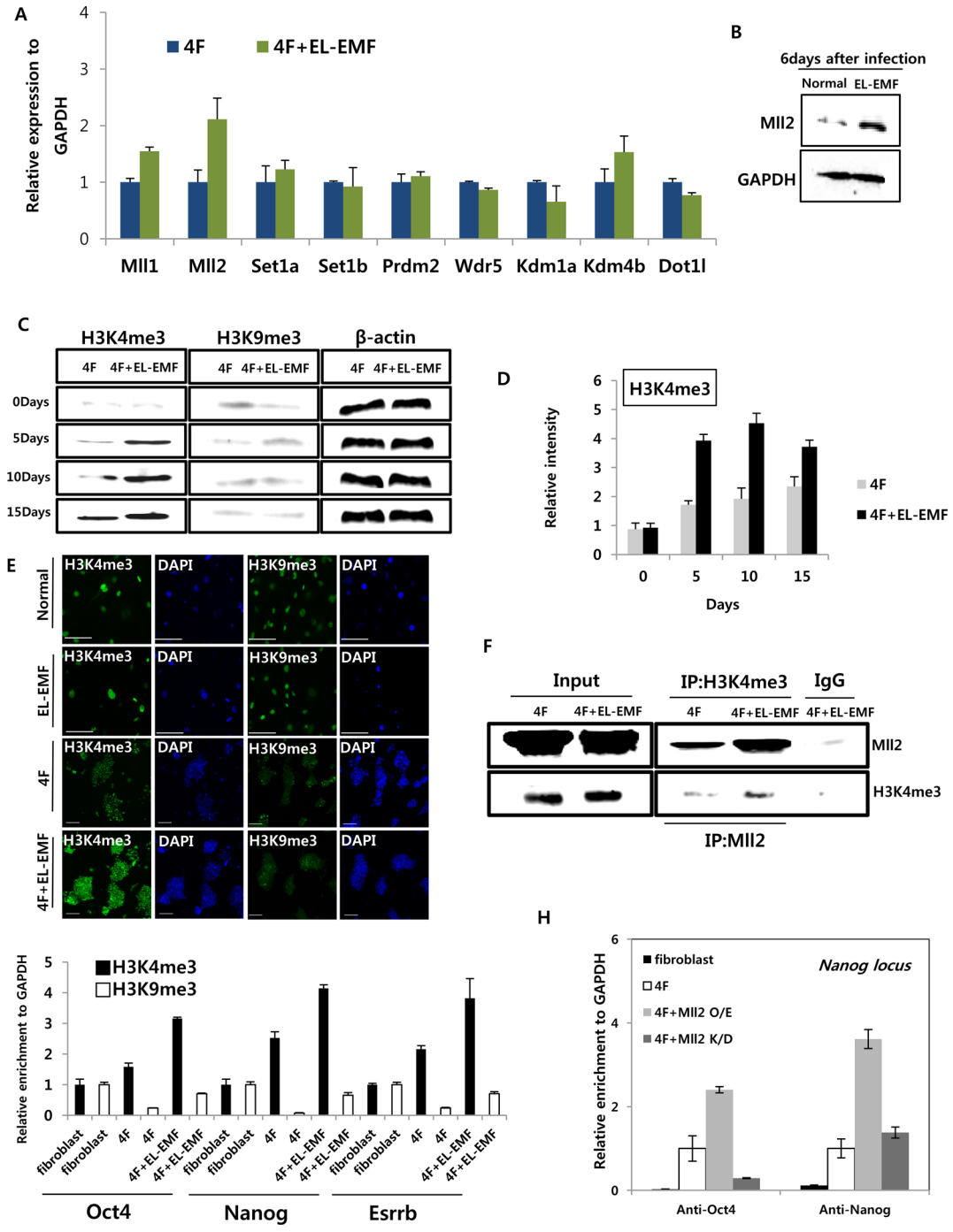

Figure 4. EL-EMF exposure during reprogramming promotes histone modifications by Mll2. (A) qRT-PCR analysis of genes related to histone modification in the presence and absence of EL-EMF exposure at 3 days after dox treatment. Two independent experiments of three sets each were performed. Data are presented as mean ± SEM; $n = 5$. (B) Western blot for Mll2 and H3K4me3 in OSKM-infected fibroblasts in the presence and absence of EL-EMF exposure. (C) Western blot analysis for H3K4me3 and H3K9me3 in OSKM-infected fibroblasts at 5, 10, and 15 days after infection. (D) Semiquantitative analysis of H3K4me3 levels in OSKM-infected fibroblasts at 5, 10, and 15 days after infection. The Western blot band intensities were measured with ImageJ software. H3K4me3 levels were normalized to β-actin levels. Three independent experiments of three sets each were performed. Data represent mean ± SEM. (E) Immunofluorescence images of histone modification markers (H3K4me3 and H3K9me3) in control fibroblasts and secondary fibroblasts in the presence and absence of EL-EMF exposure. EL-EMF exposure in secondary fibroblasts leads to significant accumulations of H3K4me3 level during the reprogramming. Scale bars: 100 μm. (F) Co-immunoprecipitation of the Mll2 and H3K4me3 complex. Co-immunoprecipitation studies carried out with lysates prepared from the secondary fibroblasts at 10 days after dox treatment. (G) H3K4me3 and H3K9me3 ChIP-PCR at Oct4, Nanog, and EsrrB promoters in secondary fibroblasts at 7 days after dox in the absence and presence of EL-EMF exposure. Three independent experiments of three sets each were performed. Data represent mean ± SEM. (H) ChIP-qPCR of Oct4 and Nanog at Nanog *locus* in reprogrammed cells, reprogramming cells combined with Mll2 overexpression and Mll2 knockdown. Three independent experiments of three sets each were performed. Data represent mean ± SEM.

dox treatment in the EL-EMF condition (Figure S4A), indicating that Mll2 may facilitate pluripotency gene activation. Interestingly, the upregulation of Mll2 and H3K4me3 levels was not observed in fibroblasts treated with EL-EMF alone (Figures 4E and S4B–D).

Mll2 is a member of trithorax (trxG) group that is mainly responsible for H3K4 trimethylation (H3K4me3) during development.[35] Thus, we measured the enrichment level of histone modifications that mark active chromatin (H3K4me3) in the EL-EMF-exposed secondary fibroblasts. Surprisingly, consistent with previous results, H3K4me3 accumulation was specific to cultures treated with EL-EMF exposure, while H3K9me3 levels were not changed by EMF exposure alone or in combination with 4 factor expression (Figures 4E and S4D). The accumulation of H3K4me3 by EL-EMF exposure was much higher than in the 4-factor-induced reprogramming at each time point in the absence of EL-EMF, suggesting that EL-EMF increases H3K4me3 levels, which then increases reprogramming efficiency (Figures 4C,D and S4E). We further found an increased interaction between Mll2 and H3K4me3 upon EL-EMF-induced reprogramming (Figure 4F), indicating that an increased H3K4me3 level is a specific effect of EL-EMF exposure. To further assess the chromatin state at pluripotency-associated loci, we performed chromatin precipitation (ChIP)-qPCR for these histone modifications. We observed that transcription start sites of Oct4, Nanog, and Esrrb are enriched for H3K4me3 in EL-EMF-exposed reprogramming cultures (Figure 4G). Taken together, these results suggest that EL-EMF-induced H3K4me3 accumulation increases accessibility of several pluripotency-associated loci during reprogramming.

Next, we investigated the consequences of increased Mll2 expression during cell reprogramming. We confirmed that Mll2 overexpression led to a significant induction in H3K4me3 levels during reprogramming (Figure S5A). Moreover, we detected increased Oct4 and Nanog binding at the Nanog locus in cultures overexpressing Mll2 at day 6 after dox treatment, and this binding could be attenuated by Mll2 depletion (Figure 4H). Consistent with this, the number of Nanog-positive colonies was markedly increased by Mll2 overexpression (Figure S5B). Conversely, suppression of Mll2 during reprogramming led to reduction in the number of Nanog-positive colonies (Figure S5B), suggesting that Mll2 governs the epigenetic reprogramming efficiency of somatic cells.

To better understand the link between EL-EMF-exposed H3K4me3 levels and reprogramming efficiency, we examined the effects of EL-EMF on reprogramming under conditions of H3K4me3 inhibition. We observed that Mll2 knockdown in EL-EMF-induced reprogramming led to significant suppression of global H3K4me3 level (Figure 5A) and reprogramming efficiency (Figure 5B). Consistent with this result, the expression of Nanog was significantly decreased by H3K4me3 inhibition on EL-EMF-induced reprogramming (Figure 5C). Furthermore, we observed that Mll2 inhibition in EL-EMF-mediated reprogramming significantly attenuates Oct4 binding at endogenous Oct4 and Nanog loci (Figure 5D).

Additionally, we asked whether Mll2-mediated EL-EMF effects the cell cycle. Lentivirus encoding Mll2 shRNA and Cre were introduced into MEF-derived from $p53^{flox/flox}$ mice.[36] We found that p53 knockout (KO) and EL-EMF resulted in significant increase in cell proliferation, and inhibition of Mll2 coupled with p53KO or EL-EMF had no negative effect on cell proliferation (Figure 5E). Despite the absence of an effect of Mll2 inhibition on cell proliferation during reprogramming in the presence of EL-EMF, Mll2 inhibition did significantly abrogate enhanced reprogramming efficiency resulting from EL-EMF exposure (Figures 5F,G and S5C). Interestingly, Mll2 inhibition had little negative effect on the increase in reprogramming efficiency resulting from p53 inhibition, which is known to be a consequence of increased cell cycling (Figures 5F,G and S5C).[29] Taken together, these results strongly suggest that Mll2-mediated EL-EMF effects on cell reprogramming are cell-cycle-independent.

Cell Reprogramming in a Magnetic-Field-Free System. The earth exists in a geomagnetic field, and as such, life on earth has evolved in the presence of this magnetic field. It is therefore very difficult to estimate the effects of the environmental magnetic field on biological systems. In order to understand the basic role of EMF in biological systems, we devised a magnetic-field-free system in the culture incubator that maintains a zero magnetic field using a three-axis Helmholtz coil (Figure S6A,B).[37] We put a three-axis sensor in the center of a Helmholtz coil, and a three-dimensional EMF generator generated reverse magnetic fields to keep a magnetic-field-free space by adjusting the voltage across the coil with a power supply (Figure S6C).

In our initial experiments, we prepared TTFs transduced with dox-inducible lentiviral vectors expressing OSKM and cultured them in the center of the three-axis Helmholtz coil (Figure 6A). Expression of pluripotency-related genes including Oct4 and Nanog was attenuated, and fibroblast-specific genes such as Dcn and Fap were not efficiently suppressed in the EMF-free system (Figure 6B). Surprisingly, we found that the EMF-free environmental system greatly delayed generation of Oct4 and Nanog-positive iPS colonies (Figure 6C). Next, we investigated histone methylation levels at pluripotency loci in the EMF-free system. Interestingly, reprogramming in the absence of EMFs resulted in significantly diminished H3K4me3 levels and slightly impeded the reduction in H3K9me3 that is known to be a barrier for reprogramming[38] at pluripotency loci including Oct4, Nanog, and Esrrb (Figure 6D,E). These results suggest that chromatin accessibility may be a rate-limiting factor for reprogramming in the EMF-free environment. By extension, this result further suggests

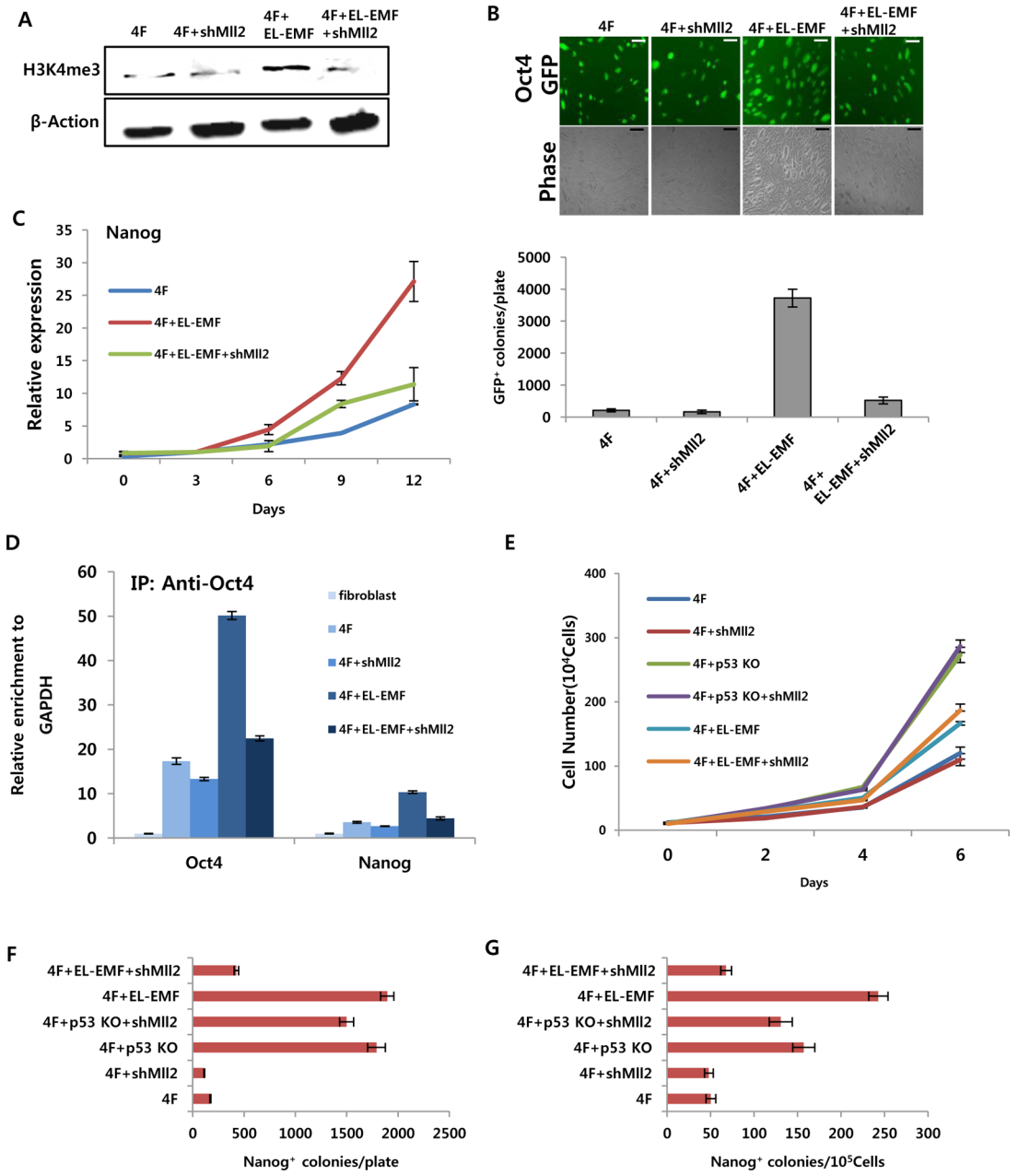

Figure 5. Mll2-mediated EL-EMF effects on reprogramming. (A) Western blot for H3K4me3 in EL-EMF-induced reprogramming in the absence and presence of Mll2 inhibition. H3K4me3 in EL-EMF-mediated reprogramming was repressed by Mll2 knockdown. (B) Representative image (top) and numbers (bottom) of *Oct4-GFP* colonies in EL-EMF-induced reprogramming in the absence and presence of Mll2 inhibition. EL-EMF-mediated reprogramming efficiency is significantly decreased by Mll2 knockdown. Three independent experiments of three sets each were performed. Data represent mean ± SEM. Scale bars: 100 μm. (C) mRNA expression of Nanog in EL-EMF-mediated reprogramming coupled with Mll2 knockdown. Three independent experiments of three sets each were performed. Data represent mean ± SEM. (D) ChIP-qPCR of Oct4 mark at Oct4 and Nanog loci in EL-EMF-mediated reprogramming coupled with Mll2 knockdown. Three independent experiments of three sets each were performed. Data represent mean ± SEM. (E) Growth curves of OSKM-infected fibroblasts in the absence and presence of EL-EMF exposure coupled with p53 knockout and Mll2 knockdown. Three independent experiments of three sets each were performed. Data represent mean ± SEM. (F) Number of Nanog-positive colonies from OSKM-infected fibroblasts in the absence and presence of EL-EMF exposure coupled with p53 knockout and Mll2 knockdown at 20 days after OSKM infection. Three independent experiments of three sets each were performed. Data represent mean ± SEM. (G) Number of Nanog-positive colonies derived from 10^5 fibroblasts in the absence and presence of EL-EMF exposure coupled with p53 knockout and Mll2 knockdown at 20 days after OSKM infection. Three independent experiments of three sets each were performed. Data represent mean ± SEM.

that the environmental electromagnetic field is a major factor for the process of epigenetic reprogramming.

In light of these findings, we cultured control ES cells (V6.5) in the EMF-free system to examine whether the absence of an EMF can influence the maintenance of pluripotency. ES cells that were exposed to EMF-free conditions for 7 days were viable and displayed typical ES cell morphology indistinguishable from control cells

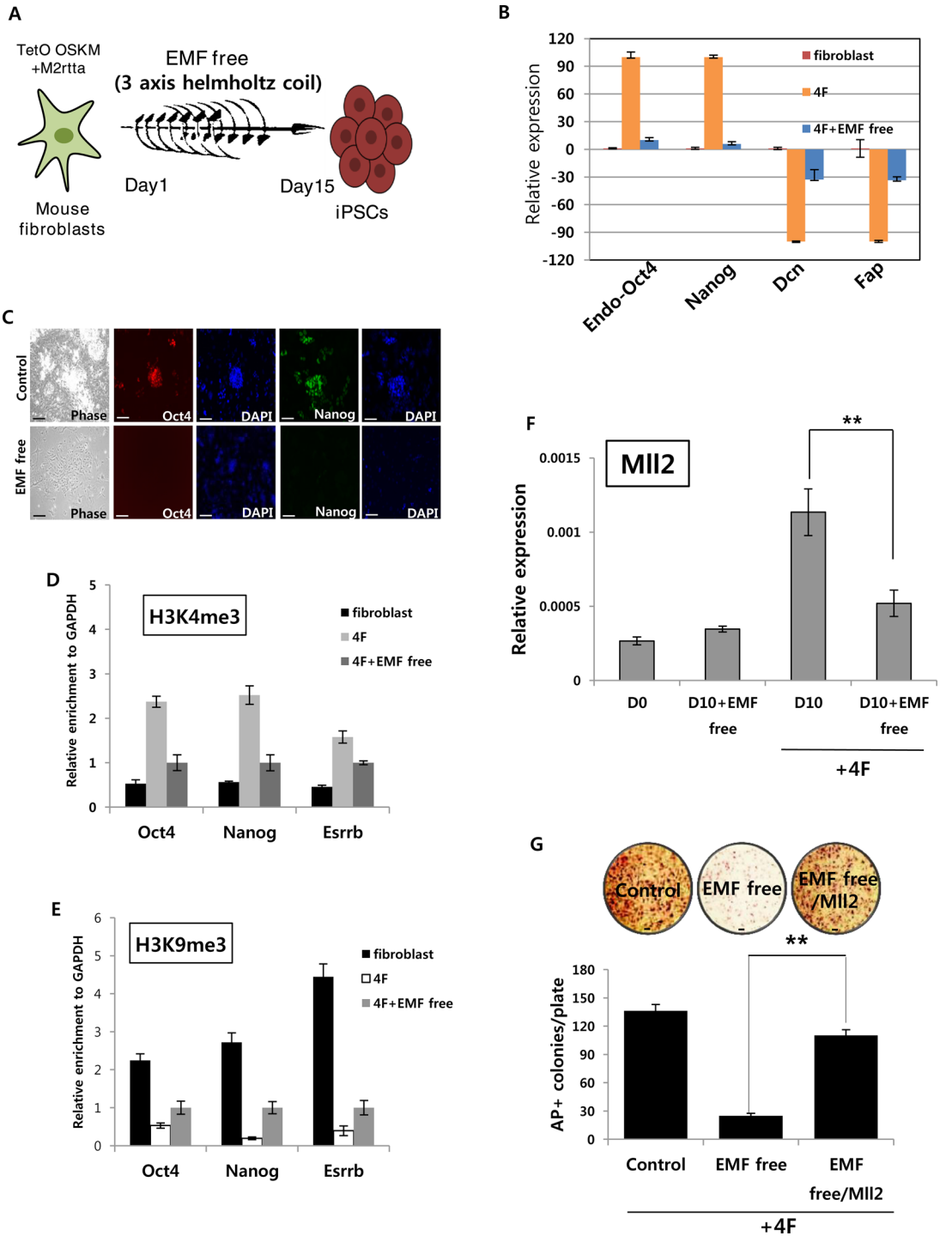

Figure 6. Earth's magnetic-field-free system inhibits epigenetic reprogramming. (A) Schematic drawing of the cell reprogramming under the EMF-free system. (B) Quantitative expression levels of pluripotency genes (Oct4, Nanog) and fibroblast-specific genes (Dcn, Fap) in cultures reprogrammed with 4 factors in the presence and absence of EMF. Three independent experiments of three sets each were performed. Data represent mean ± SEM. (C) Immunofluorescence staining for pluripotency markers, Oct4 and Nanog, reprogrammed with 4 factors in the presence and absence of environmental EMF at day15 after dox treatment. Scale bars: 100 μm. (D) H3K4me3 and (E) H3K9me3 ChIP-qPCR at pluripotency loci, Oct4, Nanog, and Esrrb in control fibroblasts and 4-factor-induced fibroblasts at 7 days after dox induction in the presence and absence of environmental EMFs. Three independent experiments of three sets each were performed. Data represent mean ± SEM. (F) mRNA expression of Mll2 under normal conditions and EMF-free conditions during reprogramming. Three independent experiments of three sets each were performed. Data represent mean ± SEM. Student *t* test, $^{**}p < 0.01$. (G) (Top) Representative image of AP staining reprogrammed cells at 20 days after OSKM infections with EMF-free and EMF-free/Mll2. (Bottom) Number of AP-positive colonies in the EMF-free and EMF-free+Mll2 during reprogramming. Overexpression of Mll2 rescues EMF-free phenotypes in the reprogramming. Three independent experiments of three sets each were performed. Data represent mean ± SEM. Student *t* test, $^{**}p < 0.01$. Scale bars: 100 μm.

(Figure S7A). Furthermore, the expression level of pluripotency genes in ES cells was unaffected in the earth's magnetic field cancellation system (Figure S7A,B), suggesting that the pluripotent state was not affected by the absence of an EMF. Additionally, fibroblasts grown in the EMF-free conditions were similarly unaffected (Figure S7C). Additionally, expressions of cell-cycle-related genes are not altered by EMF cancelation (Figure S7D).

We also observed the downregulation of Mll2 expression during iPS cell generation in the EMF-free system (Figure 6F). This observation, coupled with our prior data, suggests that the failure to induce Mll2 in the absence of EMF may prevent reprogramming through inhibiting chromatin reorganization and accessibility of the reprogramming factors to critical loci. Thus, we asked whether Mll2 overexpression could rescue cell reprogramming in the absence of EMF. Overexpression of Mll2 rescued most of the defects associated in the EMF-free system during reprogramming, increasing the number of iPS colonies (Figure 6G). These results further support a model in which the environmental magnetic field promotes chromatin reorganization through the activation of Mll2 specifically during the dynamic epigenetic changes initiated by expression of the 4 Yamanaka reprogramming factors.

CONCLUSION

As one of the fundamental forces of nature, the EMF is a physical energy produced by electrically charged objects that can affect the movement of other charged objects in the field. Here we show that this physical energy can affect cell fate changes and is essential for reprogramming to pluripotency. Exposure of cell cultures to EMFs significantly improves reprogramming efficiency in somatic cells. Interestingly, EL-EMF exposure combined with only one Yamanaka factor, Oct4, can generate iPSCs, demonstrating that EL-EMF exposure can replace Sox2, Klf4, and c-Myc during reprogramming. These results open a new possibility for a novel method for efficient generation of iPSCs. Although many chemical factors or additional genes have been reported for the generation of iPSCs, limitations such as integration of foreign genetic elements or efficiency remain a challenge.[39] Thus, EMF-induced cell fate changes may eventually provide a solution for efficient, noninvasive cell reprogramming strategies in regenerative medicine.

Interestingly, our results show that ES cells and fibroblasts themselves are not significantly affected by EMF exposure; rather, cells undergoing dramatic epigenetic changes such as reprogramming seem to be uniquely susceptible to the effects of EMFs. Consistent with this, it has been shown previously that EL-EMF is involved in the efficient neuronal development or other dynamic biological processes.[18,20,40] Consistent with this idea, we demonstrated that EL-EMF exposure increases enrichment of H3K4me3 histone modification *via* Mll2 during development and reprogramming and that this is closely associated with activation of gene expression. Importantly, the suppression of epigenetic reprogramming in EMF-free conditions indicates that EL-EMF energy is essential for favorable epigenetic remodeling during the acquisition of pluripotency.

Furthermore, we found a specific induction of Mll2 by EL-EMF exposure during reprogramming, which led to accumulation of H3K4me3, subsequently facilitating robust Oct4 and Nanog occupancy at pluripotency-regulating loci, presumably in conjunction with the trxG complex. Thus, these results describe a unique role for Mll2 in facilitating binding of the Yamanaka factors to target loci to facilitate reprogramming (Figure S8A). Additionally, downregulation of Mll2 expression in the EMF-free system during reprogramming is intriguing because these EMF-free phenotypes could be rescued by overexpression of Mll2. Thus, taken together, these data provide strong support that Mll2 is a key mediator of the effects of EMF during reprogramming. Future studies on the detailed mechanisms through which Mll2 senses EMF will provide more insight into the relationship between EMF and epigenetic plasticity.

Surprisingly, we found that an EMF-free environment was detrimental to cell fate change of epigenetic reprogramming. The earth has a substantial magnetic field, and life on Earth has evolved in the field of its naturally occurring magnetic field. It is possible that life may have evolved to utilize this magnetic field to catalyze biological processes. During cell fate determination of reprogramming, environmental EMFs may be critical for the epigenetic changes to rapidly and precisely respond to signals from the environment. Thus, these studies define the fundamental role of EMFs in establishing cellular identity of cell reprogramming, and it will be of great interest to understand the molecular mechanisms underlying the effects of EMFs on the reprogramming in the future.

MATERIALS AND METHODS

EL-EMF Exposure. We employed an EL-EMF exposure system which was previously described.[41,42] Briefly, cells were continuously exposed, for up to 30−45 days, to EL-EMF (F = 50 Hz, B_m = 1 mT) produced by a solenoid placed inside the CO_2 incubator. The device was supplied by an ac power supply (PCR-100L, Kikusui, Japan), and EF frequency and amplitude were monitored by an EF sensor (TM-701, Kanetec, Japan) connected simultaneously to a microcontroller with ADC (Atmega328p, Atmel, USA). Simulated magnetic flux density distribution by COMSOL 3.4 (COMSOL, MA) with parameters as follows: axial

symmetry (2D), radius (R 1/4 7.5 cm), current (I 1/4 200 mA), and number of loops (N 1/4 1000). Control cells were grown in a different CO_2 incubator under the same conditions without exposure to EL-EMFs. The geometry of the system assured field uniformity for the exposed cultures. The surfaces of the culture well plates were parallel to the force lines of the alternating magnetic field in the solenoid. To exclude uncontrolled thermal effects of the field during the culture, the maintenance of 37 ± 0.1C inside each exposed well was controlled by direct temperature measurement with thermometric probes. One day after infection, the fibroblasts were cultured in the EMF incubator and the cultures were moved into the normal incubator after iPSC formations.

3D Electromagnetic Field Cancellation System. The earth's magnetic field is a natural component of the environment for living organisms. The intensity of geomagnetic field is about 300−400 mG. In order to generate a zero-field environment by canceling the earth's magnetic field in the cell culture incubator, we used three-axis Helmholtz coils and the three-axis magnetic sensor (DC Miligauss Meter 3 axis, AlphaLab Inc., USA), which measures the earth's field accurately, and the system is capable of canceling the earth's field inside the three-axis Helmholtz coil. Helmholtz coils are used to generate uniform magnetic field, and each set of Helmholtz coils consists of two coils in a special arrangement to maximize the spatial volume of a uniform magnetic field. The magnetic field generated is proportional to a dc or ac current into the coil which provides a calibration curve between the field and the strength of dc current, called field-current calibration. Three-axis coils offer standard Helmholtz coils with different dimensions for generating a single-axis, two-axis, or three-axis magnetic field, and a three-dimensional EMF generator generated reverse magnetic fields to keep a magnetic-field-free space by adjusting the voltage across the coil with a power supply (PS2520G, Tektronix, USA). The cell cultures were located in the center of the three-axis Helmholtz coil in the incubator, and control cells were grown in a different CO_2 incubator under the same conditions without the Helmholtz coil.

Cell Culture. HEK293 cells were used for packaging the virus. These cells were grown in fibroblast media [high glucose DMEM (Invitrogen), 10% FBS (Hyclone), and 5% penicilin/streptomycin (Invitroge)]. These cells were co-transfected with the lentivirus construct, psPAX2, pMD2.G and tetO-OSKM/FUW-M2rtTA and OKSIM, vectors using calcium phosphate co-precipitation. Cell culture medium was replaced 24 h after transfection and virus harvested 72 h later. Mouse fibroblasts and human dermal fibroblasts were transduced (40 000 cells) at passage 2 or 3 in 6-well culture dishes with the lentivirus. Infected mouse fibroblasts were cultured in mESC media with dox (2 μg/mL), and human fibroblasts were cultured in hESC media.[43] The "2i" including ERK(PD0325901) and GSK3b inhibitor (CHIR99021) was purchased from LC biolab. VPA was purchased from Sigma-Aldrich. Drugs' working concentration: bVPA (1 mM), Vc (30 μg/mL), PD0325901 (1 μM), CHIR99021 (3 μM).

Alkaline Phosphatase Staining. Alkaline phosphatase staining was performed using an alkaline phosphatase substrate kit (Millipore) according to manufacturer's recommendations. For the number of AP+ colonies, equal numbers of cells were plated on 100 mm dishes coated with gelatin. Experiments were repeated three times, and data represented the mean of triplicate wells ± SEM.

Immunofluorescence Analysis. iPS cells were cultured on pretreated coverslips, fixed with 4% PFA. The cells were then stained with primary antibodies against human/mouse Oct4 (Santa Cruz), mouse Nanog (Bethyl Lab), H3K4me3 (Abcam), H3K9me3 (Abcam), H3K27me3 (Millipore), human TRA-1-60 (Millipore), human/mouse Sox2 (R&D), and human Nanog (R&D). Respective secondary antibodies were conjugated to Alexa Fluor (Invitrogen). Nuclei were counterstained with 4,6-diamidino-2-phenylindole (DAPI; Invitrogen). Cells were imaged with a Nikon eclipse Ti. The two-color images were saved as a tif file format and merged with Adobe Photoshop software.

Flow Cytometry. All flow cytometry was performed on a C6 cytometer (Accuri). Data were analyzed with FlowJo software (TreeStar). Briefly, cells were dissociated with trypsin for 5 min, and single cells were then pelleted, resuspended in ice-cold 4% paraformaldehyde, and incubated for 10 min at 4 °C. The cells were washed twice and resuspended in FACS buffer for analysis on a FACS analyzer.

Western Blot. Western blot was carried out as described previously.[44]

PCR Analysis. For quantitative PCR (qPCR) analysis, RNA was isolated using a purelink RNA mini kit (Ambion). Complementary DNA was produced with the Super Script III kit (Invitrogen). Real-time quantitative PCR reactions were set up in triplicate with the SYBR FAST qPCR Kit (KAPA) and run on a step-one plus real-time PCR system (Applied Biosystem). Gene expression data were presented as relative expression to *GAPDH*. Primer sequence: previously described mouse primer sequence[22] was employed. Human primers were purchased from an Allele iPSC RT-PCR primer set (CAT# ABP-SC-iPShRES).

Chromatin Immunoprecipitation (ChIP)-qPCR. 2′MEFs, reprogramming intermediates, and iPS cells (7×10^6) were collected for ChIP analysis performed using the enzymatic chromatin IP kit (cell signaling) per the manufacturer's instructions. Primer sequence wasa from a previous report.[45]

Bisulfite Sequencing. Bisulfite sequencing was performed according to a method previously described.[42,46] Briefly, bisulfite reactions were carried out according to the manufacturer's instructions (Epitect bisulfite kit, Qiagen). Two to four microliters of bisulfite-treated DNA was used in a standard PCR protocol to amplify Oct4 and Nanog promoter regions in mouse V6.5 ES cells, fibroblasts, and iPS cells. PCR products were cloned into the pCR2.1 vector (Invitrogen) and sequenced using the M13.

Generation of Teratomas and Chimeras. iPS cells were collected and separated from feeders by sedimentation of iPS cell aggregates. Cells were washed, resuspended in 500 μL of mouse ES cell medium, and injected subcutaneously into SCID mice (Taconic). Four weeks after injection, tumors were removed from euthanized mice and fixed in formalin. Samples were paraffin-imbedded, sectioned, and analyzed on the basis of hematoxylin and eosin staining. For blastocyst injections, iPSCs were injected into B6XDBA F2 host blastocysts as described previously.[46]

Conflict of Interest: The authors declare no competing financial interest.

Acknowledgment. This work was supported by the National Research Foundation of Korea funded by the Ministry of Education, Science, and Technology (NRF-2009-0082941, NRF-2013R1A1A1058835, NRF-2013M3A9B4076485, NRF-2013M3A9B4044387), Korea Health Technology R&D Project, Ministry of Health & Welfare (HI13C0540), and the Next-Generation BioGreen 21 Program, Rural Development Administration (PJ009073).

Supporting Information Available: Supplementary Figure 1: EL-EMF exposure enhances cell reprogramming. Supplementary Figure 2: Characterization of EL-EMF-induced iPSCs. Supplementary Figure 3: Characterization of Oct4- and EL-EMF-induced iPSCs. Supplementary Figure 4: Histone modifications by EL-EMF exposure during reprogramming. Supplementary Figure 5: Mll2 facilitates efficient cell reprogramming. Supplementary Figure 6: EMF cancellation system. Supplementary Figure 7: Somatic cell reprogramming under EMF-free system. Supplementary Figure 8: Schematic representation of EL-EMF-mediated reprogramming. Somatic cell reprogramming under EMF-free system. This material is available free of charge *via* the Internet at http://pubs.acs.org.

REFERENCES AND NOTES

1. Hollenbach, D. F.; Herndon, J. M. Deep-Earth Reactor: Nuclear Fission, Helium, and the Geomagnetic Field. *Proc. Natl. Acad. Sci. U.S.A.* **2001**, *98*, 11085–11090.
2. Lacy-Hulbert, A.; Metcalfe, J. C.; Hesketh, R. Biological Responses to Electromagnetic Fields. *FASEB J.* **1998**, *12*, 395–420.
3. Doucet, I. L. Biological Effects of Low Frequency Electromagnetic Fields. *Med. War* **1992**, *8*, 205–212.

4. Arendash, G. W.; Sanchez-Ramos, J.; Mori, T.; Mamcarz, M.; Lin, X.; Runfeldt, M.; Wang, L.; Zhang, G.; Sava, V.; Tan, J.; *et al.* Electromagnetic Field Treatment Protects Against and Reverses Cognitive Impairment in Alzheimer's Disease Mice. *J. Alzheimer's Dis.* **2010**, *19*, 191–210.
5. Caprani, A.; Richert, A.; Flaud, P. Experimental Evidence of a Potentially Increased Thrombo-Embolic Disease Risk by Domestic Electromagnetic Field Exposure. *Bioelectromagnetics* **2004**, *25*, 313–315.
6. Danilenko, S. R.; Shatrov, A. A.; Gerasimovich, O. I. The Efficacy of Using an Electromagnetic Field of Extremely High Frequency (54−78 GHz) in Treating Patients with Chronic Nonspecific Lung Disease. *Vopr. Kurortol., Fizioter. Lech. Fiz. Kul't.* **1995**, 16–18.
7. Sadlonova, J.; Korpas, J.; Vrabec, M.; Salat, D.; Buchancova, J.; Kudlicka, J. The Effect of the Pulsatile Electromagnetic Field in Patients Suffering from Chronic Obstructive Pulmonary Disease and Bronchial Asthma. *Bratisl. Lek. Listy* **2002**, *103*, 260–265.
8. Bakhmutskii, N. G.; Golubtsov, V. I.; Pyleva, T. A.; Sinitskii, D. A.; Frolov, V. E. A Case of Successful Treatment of a Patient with Breast Cancer Using Rotational Electromagnetic Field. *Sov. Med.* **1991**, 86–87.
9. Del Vecchio, G.; Giuliani, A.; Fernandez, M.; Mesirca, P.; Bersani, F.; Pinto, R.; Ardoino, L.; Lovisolo, G. A.; Giardino, L.; Calza, L. Effect of Radiofrequency Electromagnetic Field Exposure on *In Vitro* Models of Neurodegenerative Disease. *Bioelectromagnetics* **2009**, *30*, 564–572.
10. Wang, Q.; Wu, W.; Chen, X.; He, C.; Liu, X. Effect of Pulsed Electromagnetic Field with Different Frequencies on the Proliferation, Apoptosis and Migration of Human Ovarian Cancer Cells. *Shengwu Yixue Gongchengxue Zazhi* **2012**, *29*, 291–295.
11. Maaroufi, K.; Save, E.; Poucet, B.; Sakly, M.; Abdelmelek, H.; Had-Aissouni, L. Oxidative Stress and Prevention of the Adaptive Response to Chronic Iron Overload in the Brain of Young Adult Rats Exposed to a 150 Kilohertz Electromagnetic Field. *Neuroscience* **2011**, *186*, 39–47.
12. Ceccarelli, G.; Bloise, N.; Mantelli, M.; Gastaldi, G.; Fassina, L.; De Angelis, M. G.; Ferrari, D.; Imbriani, M.; Visai, L. A Comparative Analysis of the *In Vitro* Effects of Pulsed Electromagnetic Field Treatment on Osteogenic Differentiation of Two Different Mesenchymal Cell Lineages. *BioRes. Open Access* **2013**, *2*, 283–294.
13. An, G. Z.; Zhou, Y.; Hou, Q. X.; Li, Y. R.; Jiang, D. P.; Guo, G. Z.; Zhang, C.; Ding, G. R. Effect of Long-Term Power Frequency Electromagnetic Field Exposure on Proliferation and Apoptosis of SRA01/04 Cells. *Zhonghua Laodong Weisheng Zhiyebing Zazhi* **2013**, *31*, 246–250.
14. Seong, Y.; Moon, J.; Kim, J. Egr1 Mediated the Neuronal Differentiation Induced by Extremely Low-Frequency Electromagnetic Fields. *Life Sci.* **2014**, *102*, 16–27.
15. Juutilainen, J. Developmental Effects of Electromagnetic Fields. *Bioelectromagnetics* **2005**, *26*, S107–S115.
16. Hotary, K. B.; Robinson, K. R. Endogenous Electrical Currents and the Resultant Voltage Gradients in the Chick Embryo. *Dev. Biol.* **1990**, *140*, 149–160.
17. Levin, M. Large-Scale Biophysics: Ion Flows and Regeneration. *Trends Cell Biol.* **2007**, *17*, 261–270.
18. Hiraki, Y.; Endo, N.; Takigawa, M.; Asada, A.; Takahashi, H.; Suzuki, F. Enhanced Responsiveness to Parathyroid Hormone and Induction of Functional Differentiation of Cultured Rabbit Costal Chondrocytes by a Pulsed Electromagnetic Field. *Biochim. Biophys. Acta* **1987**, *931*, 94–100.
19. Kang, K. S.; Hong, J. M.; Kang, J. A.; Rhie, J. W.; Jeong, Y. H.; Cho, D. W. Regulation of Osteogenic Differentiation of Human Adipose-Derived Stem Cells by Controlling Electromagnetic Field Conditions. *Exp. Mol. Med.* **2013**, *45*, e6.
20. Meng, D.; Xu, T.; Guo, F.; Yin, W.; Peng, T. The Effects of High-Intensity Pulsed Electromagnetic Field on Proliferation and Differentiation of Neural Stem Cells of Neonatal Rats *In vitro*. *J. Huazhong Univ. Sci. Technol., Med. Sci.* **2009**, *29*, 732–736.
21. Pesce, M.; Patruno, A.; Speranza, L.; Reale, M. Extremely Low Frequency Electromagnetic Field and Wound Healing: Implication of Cytokines as Biological Mediators. *Eur. Cytokine Network* **2013**, *24*, 1–10.
22. Takahashi, K.; Yamanaka, S. Induction of Pluripotent Stem Cells from Mouse Embryonic and Adult Fibroblast Cultures by Defined Factors. *Cell* **2006**, *126*, 663–676.
23. Lengner, C. J.; Camargo, F. D.; Hochedlinger, K.; Welstead, G. G.; Zaidi, S.; Gokhale, S.; Scholer, H. R.; Tomilin, A.; Jaenisch, R. Oct4 Expression Is Not Required for Mouse Somatic Stem Cell Self-Renewal. *Cell Stem Cell* **2007**, *1*, 403–415.
24. Carey, B. W.; Markoulaki, S.; Hanna, J.; Saha, K.; Gao, Q.; Mitalipova, M.; Jaenisch, R. Reprogramming of Murine and Human Somatic Cells Using a Single Polycistronic Vector. *Proc. Natl. Acad. Sci. U.S.A.* **2009**, *106*, 157–162.
25. Maherali, N.; Sridharan, R.; Xie, W.; Utikal, J.; Eminli, S.; Arnold, K.; Stadtfeld, M.; Yachechko, R.; Tchieu, J.; Jaenish, R.; *et al.* Directly Reprogrammed Fibroblasts Show Global Epigenetic Remodeling and Widespread Tissue Contribution. *Cell Stem Cell* **2007**, *1*, 55–70.
26. Esteban, M. A.; Wang, T.; Qin, B.; Yang, J.; Qin, D.; Cai, J.; Li, W.; Weng, Z.; Chen, J.; Ni, S.; *et al.* Vitamin C Enhances the Generation of Mouse and Human Induced Pluripotent Stem Cells. *Cell Stem Cell* **2010**, *6*, 71–79.
27. Huangfu, D.; Maehr, R.; Guo, W.; Eijkelenboom, A.; Snitow, M.; Chen, A. E.; Melton, D. A. Induction of Pluripotent Stem Cells by Defined Factors is Greatly Improved by Small-Molecule Compounds. *Nat. Biotechnol.* **2008**, *26*, 795–797.
28. Wernig, M.; Lengner, C. J.; Hanna, J.; Lodato, M. A.; Steine, E.; Foreman, R.; Staerk, J.; Markoulaki, S.; Jaenisch, R. A Drug-Inducible Transgenic System for Direct Reprogramming of Multiple Somatic Cell Types. *Nat. Biotechnol.* **2008**, *26*, 916–924.
29. Hanna, J.; Saha, K.; Pando, B.; van Zon, J.; Lengner, C. J.; Creyghton, M. P.; van Oudenaarden, A.; Jaenisch, R. Direct Cell Reprogramming Is a Stochastic Process Amenable to Acceleration. *Nature* **2009**, *462*, 595–601.
30. Antony, J.; Oback, F.; Chamley, L. W.; Oback, B.; Laible, G. Transient JMJD2B-Mediated Reduction of H3K9me3 Levels Improves Reprogramming of Embryonic Stem Cells into Cloned Embryos. *Mol. Cell. Biol.* **2013**, *33*, 974–983.
31. Mansour, A. A.; Gafni, O.; Weinberger, L.; Zviran, A.; Ayyash, M.; Rais, Y.; Krupalnik, V.; Zerbib, M.; Amann-Zalcenstein, D.; Maza, I.; *et al.* The H3K27 Demethylase Utx Regulates Somatic and Germ Cell Epigenetic Reprogramming. *Nature* **2012**, *488*, 409–413.
32. Mattout, A.; Biran, A.; Meshorer, E. Global Epigenetic Changes During Somatic Cell Reprogramming to iPS Cells. *J. Mol. Cell Biol.* **2011**, *3*, 341–350.
33. Belyaev, I. Y.; Hillert, L.; Protopopova, M.; Tamm, C.; Malmgren, L. O.; Persson, B. R.; Selivanova, G.; Harms-Ringdahl, M. 915 MHz Microwaves and 50 Hz Magnetic Field Affect Chromatin Conformation and 53BP1 Foci in Human Lymphocytes from Hypersensitive and Healthy Persons. *Bioelectromagnetics* **2005**, *26*, 173–184.
34. Zhang, Y.; She, F.; Li, L.; Chen, C.; Xu, S.; Luo, X.; Li, M.; He, M.; Yu, Z. p25/CDK5 Is Partially Involved in Neuronal Injury Induced by Radiofrequency Electromagnetic Field Exposure. *Int. J. Radiat. Biol.* **2013**, *89*, 976–984.
35. FitzGerald, K. T.; Diaz, M. O. MLL2: A New Mammalian Nember of the Trx/MLL Family of Genes. *Genomics* **1999**, *59*, 187–192.
36. Marino, S.; Vooijs, M.; van Der Gulden, H.; Jonkers, J.; Berns, A. Induction of Medulloblastomas in p53-null Mutant Mice by Somatic Inactivation of Rb in the External Granular Layer Cells of The Cerebellum. *Genes Dev.* **2000**, *14*, 994–1004.
37. Gyawali, S. R. Design and Construction of Helmholtz Coil for Biomagnetic Studies on Soybean, University of Missouri—Columbia, 2008.
38. Chen, J.; Liu, H.; Liu, J.; Qi, J.; Wei, B.; Yang, J.; Liang, H.; Chen, Y.; Chen, J.; Wu, Y.; *et al.* H3K9 Methylation Is a Barrier during Somatic Cell Reprogramming Into iPSCs. *Nat. Genet.* **2013**, *45*, 34–42.
39. Feng, B.; Ng, J. H.; Heng, J. C.; Ng, H. H. Molecules That Promote or Enhance Reprogramming of Somatic Cells to Induced Pluripotent Stem Cells. *Cell Stem Cell* **2009**, *4*, 301–312.

40. Berg, H. Problems of Weak Electromagnetic Field Effects in Cell Biology. *Bioelectrochem. Bioenerg.* **1999**, *48*, 355–360.
41. Loginov, V. A. Accumulation of Calcium Ions in Myocardial Sarcoplasmic Reticulum of Restrained Rats Exposed to the Pulsed Electromagnetic Field. *Aviakosm. Ekol. Med.* **1992**, *26*, 49–51.
42. Cho, H.; Seo, Y. K.; Yoon, H. H.; Kim, S. C.; Kim, S. M.; Song, K. Y.; Park, J. K. Neural Stimulation on Human Bone Marrow-Derived Mesenchymal Stem Cells by Extremely Low Frequency Electromagnetic Fields. *Biotechnol. Prog.* **2012**, *28*, 1329–1335.
43. Takahashi, K.; Tanabe, K.; Ohnuki, M.; Narita, M.; Ichisaka, T.; Tomoda, K.; Yamanaka, S. Induction of Pluripotent Stem Cells from Adult Human Fibroblasts by Defined Factors. *Cell* **2007**, *131*, 861–872.
44. Mahmood, T.; Yang, P. C. Western Blot: Technique, Theory, and Trouble Shooting. *North Am. J. Med. Sci.* **2012**, *4*, 429–34.
45. Doege, C. A.; Inoue, K.; Yamashita, T.; Rhee, D. B.; Travis, S.; Fujita, R.; Guarnieri, P.; Bhagat, G.; Vanti, W. B.; Shih, A.; *et al.* Early-Stage Epigenetic Modification during Somatic Cell Reprogramming by Parp1 and Tet2. *Nature* **2012**, *488*, 652–625.
46. Kim, J.; Lengner, C. J.; Kirak, O.; Hanna, J.; Cassady, J. P.; Lodato, M. A.; Wu, S.; Faddah, D. A.; Steine, E. J.; Gao, Q.; *et al.* Reprogramming of Postnatal Neurons into Induced Pluripotent Stem Cells by Defined Factors. *Stem Cells* **2011**, *29*, 992–1000.